

Van der Waals model of adsorption

D. E. Sullivan

Department of Physics, University of Guelph, Guelph, Ontario N1G 2W1, Canada

(Received 14 June 1979)

A statistical-mechanical model for physical adsorption of a gas on a solid substrate is developed, based on Van der Waals' concept of dividing the interaction potential between a pair of molecules into a hard-sphere repulsive part and an infinitely weak and long-range attractive part. The interaction between the substrate and gas molecules is similarly modeled by a hard-wall repulsive potential with long-range attractive tail. For a specific choice of the intermolecular and wall-molecule attractive terms, an explicit solution is obtained for the model. This solution shows that three different classes of adsorption isotherm are possible: in class I, the adsorption is infinite in the limit that the gas pressure approaches the saturated vapor pressure, in class II the adsorption remains finite in the limit, while in class III the adsorption becomes negative in the limit. If the temperature of crossover between different classes is plotted as a function of ϵ_w/α , where ϵ_w and α are respectively the minimum of the wall-molecule potential and the integrated strength of intermolecular attractions, then the resulting curve has the same shape as the bulk phase coexistence curve. The model shows agreement with experimental results for the adsorption of argon, krypton, and xenon on graphite, and for argon adsorbed on xenon, as well as with recent computer-simulation results for argon adsorbed on carbon dioxide.

I. INTRODUCTION

In this paper we examine a simple model of a gas interacting with a solid substrate. Our main purpose is to provide a statistical-mechanical interpretation of the observation, recently made by Dash^{1,2} and by Peierls,³ that adsorbed films exhibit three different classes of growth behavior. In films of class I, the amount of adsorbed material becomes infinite in the limit that the pressure reaches the saturated vapor pressure; in class-II films, the adsorption is finite in the limit; in class III, no adsorption occurs at all. While the work in Refs. 1-3 shows that the existence of the three modes of growth can be deduced on thermodynamic grounds alone, the present approach permits us to classify the behavior of a film directly from knowledge of a few parameters, namely the temperature and the relative strengths of the intermolecular and gas-substrate potentials. The existence and location of crossovers between different classes follows directly. In particular, the model predicts that a given material will change from class-II behavior to either class I or class III as the temperature is increased.

The model fluid examined here consists of molecules interacting with each other through a pair potential containing a hard-sphere repulsive core as well as a very weak and long-range attractive tail. The fluid is bounded in one direction by a planar impenetrable wall, which may also have a long-range attractive interaction with the molecules. Thermodynamically, it is well known that the model leads to Van der Waals's equation of state.⁴ In applying the model to an inhomogeneous

fluid, we follow here a formulation originally due to Van Kampen⁵ and subsequently used in a discussion of the liquid-gas interface by Percus.⁶ The present treatment generalizes some earlier work of ours^{7b} which dealt only with a hard repulsive wall potential.

After reviewing the model in Sec. II, we describe its solution in Sec. III. This is achieved analytically by adopting particular forms both for the attractive tail of the pair potential and for the attractive part of the wall-molecule potential. The existence of three different modes of growth then follows explicitly. It is further shown that the "crossover curve," i.e., the relation between the temperature at which a film changes classes and the ratio of the wall-molecule potential minimum to the integrated strength of intermolecular attractions, has the same shape as the bulk phase coexistence curve. This result may well have a domain of validity beyond the context of the Van der Waals model. While the use of alternative forms for the interaction potentials would likely change some details of the solution, the extreme assumption of infinitely long-range attractions precludes adopting forms for these potentials which faithfully approximate realistic models of interest (e.g., Lennard-Jones). The present model is therefore best viewed in the same light as Van der Waals's model for bulk fluids, that is, providing a useful and qualitatively correct description of fluid condensation in the presence of surfaces; with suitable adjustment of the parameters of the model, it may indeed prove to be quantitatively usable.⁴

One serious limitation at present to the Van der

Waals model, in attempting to make quantitative comparisons with experiment, is that it is restricted to describing disordered fluid phases. Thus it makes no allowance for the formation of solidlike adsorbed layers with their accompanying distinctively "stepped" adsorption isotherms.⁸ Application of the theory is also restricted by the still rather limited extent of reliably known gas-surface potential well depths. For this reason, we do not attempt to compare the model with two recent studies, of ammonia⁹ and ethylene¹⁰ adsorbed on graphite, which show clearly the crossover from class-II to class-I films with increasing temperature. Here we confine ourselves to making predictions concerning the adsorption of rare gases: While the crossover regions for these gases on bare graphite surfaces have not yet been measured, the model does accord with results for the adsorption of argon on preadsorbed layers of xenon,¹¹ as discussed in Sec. IV. A further test of the model is provided by recent Monte Carlo work,¹² simulating the adsorption of argon on carbon dioxide. For the same temperatures and potentials used in Ref. 12, the Van der Waals model predicts the formation of class-II films, in agreement with the simulation results. These findings contradict an earlier "density-functional" theory,^{13,14} which predicts class-I film formation in this case. The results obtained here underline the deficiencies of the density-functional and other related theories,^{15,16} on which we comment further in Sec. V, where we also discuss possible extensions of the present treatment.

II. MODEL

The Van der Waals model for nonuniform fluids¹⁻⁶ is based on the standard division of the intermolecular pair potential into two parts: a short-range repulsive part, here taken to be the hard-sphere interaction, and an attractive part $w_2(r)$. The latter is assumed to be very weak and long ranged. These properties may be characterized by introducing an inverse range parameter γ , such that

$$w_2(r) = \gamma^\nu \Phi(\gamma r), \quad \gamma \rightarrow 0, \quad (1)$$

where ν is the dimensionality. In the $\gamma \rightarrow 0$ limit, a molecule at position \vec{r} sees these attractive forces only via an *effective* external potential

$$\Delta\phi_{\text{eff}}(\vec{r}) = \int d^{\nu}\vec{r}' w_2(|\vec{r} - \vec{r}'|) \rho(\vec{r}'), \quad (2)$$

where $\rho(\vec{r})$ is the average position-dependent number density and where fluctuations of the density over the length scale γ^{-1} have been neglected.⁶ This result, that the attractive pair forces mani-

fest themselves only through an effective potential, demonstrates the essential mean-field nature of the Van der Waals model.

One is now left with determining the properties of a hard-sphere fluid at total chemical potential μ and in the presence of a total effective external potential

$$\phi_{\text{eff}}(\vec{r}) = \phi(\vec{r}) + \Delta\phi_{\text{eff}}(\vec{r}), \quad (3)$$

where $\phi(\vec{r})$ is any imposed potential that may be present. Further analysis depends on the behavior of $\phi(\vec{r})$. Suppose first that this function is only slowly varying, i.e., on the scale γ^{-1} . If it is then *assumed* that $\rho(\vec{r})$ is only slowly varying, it follows from (1) and (2) that $\Delta\phi_{\text{eff}}(\vec{r})$ varies on the scale γ^{-1} and hence that the total potential $\phi_{\text{eff}}(\vec{r})$ is only slowly varying. But in this case it can be shown, both asymptotically¹⁷ and rigorously,¹⁸ that the properties of the nonuniform hard-sphere system are determined in the $\gamma \rightarrow 0$ limit by the local balance of potentials:

$$\mu - \phi_{\text{eff}}(\vec{r}) = \mu_h\{\rho(\vec{r})\}. \quad (4)$$

Here $\mu_h\{\rho(\vec{r})\}$ is the bulk chemical potential of hard spheres evaluated at the local density $\rho(\vec{r})$. This result verifies the original assumption that $\rho(\vec{r})$ varies on the scale γ^{-1} . Note that in a system of uniform density $\rho(\vec{r}) = \rho$ [imposed potential $\phi(\vec{r}) = 0$], Eq. (4) becomes

$$\mu + \alpha\rho = \mu_h, \quad (5)$$

where $\mu_h \equiv \mu_h(\rho)$ and

$$\alpha \equiv - \int d^{\nu}\vec{r} w_2(r) = - \int d^{\nu}\vec{x} \Phi(|\vec{x}|), \quad (6)$$

where the second equality in (6) follows using Eq. (1). Equation (5) leads to a generalized⁴ Van der Waals expression for the pressure p ,

$$p = p_h - \frac{\alpha}{2} \rho^2, \quad (7)$$

where p_h is the pressure due to hard spheres at density ρ .

The "local thermodynamic" relation (4) is obtained in the $\gamma \rightarrow 0$ limit on assuming that the imposed potential $\phi(\vec{r})$ varies only on the scale γ^{-1} . In the particular case $\phi(r) = 0$ everywhere, a nonuniform density may still result due to separation into coexisting phases. Equation (4) can be used to show that in this instance the equation of state (7) of the separate uniform phases must be supplemented by the Maxwell equal-area construction.⁵ The interfacial density profile between the coexisting phases can also be described.⁶

When we turn to examine a fluid bounded by a wall, the latter representing for example a solid substrate, it is certainly no longer true that $\phi(\vec{r})$

and $\rho(\vec{r})$ are everywhere slowly varying. Considering in particular a planar impenetrable wall located (in three dimensions) in the x - y plane at $z = 0$, with fluid occupying the region $z > 0$, it is clear that $\rho(\vec{r})$ and $\phi(\vec{r})$ must satisfy

$$\left. \begin{aligned} \phi(\vec{r}) &= \infty \\ \rho(\vec{r}) &= 0 \end{aligned} \right\} z < 0. \quad (8)$$

We shall here suppose that $\phi(\vec{r})$ for $z > 0$ varies only on the scale γ^{-1} . Further, taking this variation to be only in the z direction, we therefore set

$$\phi(\vec{r}) = \phi_L(\gamma z), \quad z > 0. \quad (9)$$

The potential $\phi_L(\gamma z)$ may represent, for instance, the attractive field of the substrate on the fluid molecules.

Consistent with (8) and (9), the density profile will vary only in the z direction, i.e., $\rho(\vec{r}) = \rho(z)$. The abrupt change in $\phi(\vec{r})$ at $z = 0$, however, causes $\rho(z)$ for $z > 0$ to undergo short-range (compared with γ^{-1}) oscillations. These oscillations can be accurately described by analytic models^{19,20} in the case of hard spheres at a hard wall, where both $\phi_L(\gamma z)$ and $w_2(r)$ are zero. Thus, generally we must allow that^{7b}

$$\rho(z) = [\Delta\rho_s(z) + \rho_L(\gamma z)] \theta(z), \quad (10)$$

where $\theta(z)$ is the unit step function. Here $\rho_L(\gamma z)$ contains those components of the density profile which vary for $z > 0$ on the scale γ^{-1} , and approaches the asymptotic uniform value ρ as $z \rightarrow \infty$. The remaining contributions to the density profile are included in $\Delta\rho_s(z)$, which is assumed to decay to zero as $z \rightarrow \infty$ more rapidly than γ^{-1} . When (10) is used in Eq. (2) to evaluate the effective potential $\Delta\phi_{\text{eff}}(\vec{r})$, the contribution due to $\Delta\rho_s(z)$ will be a function proportional to γ and so can be neglected in the $\gamma \rightarrow 0$ limit. Therefore, taking account of (1), $\Delta\phi_{\text{eff}}(\vec{r}) = \Delta\phi_{\text{eff}}(\gamma z)$ is given by

$$\Delta\phi_{\text{eff}}(\gamma z) = \int d^3(\gamma\vec{r}') \Phi(\gamma|\vec{r} - \vec{r}'|) \rho_L(\gamma z') \Theta(\gamma z'). \quad (11)$$

There remains the determination of the density profile $\rho(z)$ of hard spheres in the total potential $\phi_{\text{eff}}(\vec{r})$, subject to the boundary condition $\rho(z) = 0$ for $z < 0$. It must also be verified that the solution for $\rho(z)$ is consistent with Eq. (10) in the $\gamma \rightarrow 0$ limit. This analysis can be carried out explicitly for a one-dimensional system: The nature of the results leads us to suggest, without proof, that they are true more generally. In that case, in the $\gamma \rightarrow 0$ limit, the slowly varying part $\rho_L(\gamma z)$ is again found to be the solution to local thermodynamics:

$$\left. \begin{aligned} \mu - \phi_{\text{eff}}(\gamma z) &= \mu_h[\rho_L(\gamma z)], \\ \phi_{\text{eff}}(\gamma z) &= \phi_L(\gamma z) + \Delta\phi_{\text{eff}}(\gamma z) \end{aligned} \right\} z > 0. \quad (12)$$

The short-range part $\Delta\rho_s(z)$, on the other hand, is given by^{7b}

$$\begin{aligned} \Delta\rho_s(z) &= \rho_s(z) - \rho_a, \quad z > 0 \\ \rho_a &= \rho_L(0), \end{aligned} \quad (13)$$

where $\rho_s(z)$ is the density profile of hard spheres at a hard wall, corresponding to an asymptotic bulk density ρ_a . Equations (11) and (12) show that $\rho_L(\gamma z)$ can be treated independently of $\rho_s(z)$. In contrast, the latter depends crucially, via ρ_a , on the behavior of $\rho_L(\gamma z)$. In the following, however, we shall only be concerned with obtaining $\rho_L(\gamma z)$.

It is worth pointing out, as we have mentioned in previous work,⁷ the profound difference between the behavior of the microscopic structure of the bulk uniform fluid, as measured by the pair correlation function, and the behavior of the surface structure indicated by the density profile, in the Van der Waals or $\gamma \rightarrow 0$ limit. In this limit, the microscopic structure of the bulk fluid is simply that of the reference fluid interacting by hard-sphere forces alone.⁴ In contrast, as seen above, the effect of the γ -parametrized attractive intermolecular forces on the surface structure is certainly nonnegligible in the $\gamma \rightarrow 0$ limit.

III. SOLUTION FOR $\rho_L(\gamma z)$

The Van der Waals model for the structure of a fluid near a wall is given by the solution to Eqs. (11) and (12). Here we solve these equations using a particular choice for the imposed external potential $\phi_L(\gamma z)$ and for the attractive part $\Phi(\gamma r)$ of the pair potential. For the external potential, we take

$$\phi_L(\gamma z) = -\epsilon_w e^{-\gamma z}, \quad (14)$$

where the parameter ϵ_w measures the well depth for wall-molecule interactions. The form of pair potential that we choose actually depends on dimensionality. In one dimension, this is

$$\Phi(\gamma r) = -\frac{\alpha}{2} e^{-\gamma r}, \quad (15a)$$

while in three dimensions we take

$$\Phi(\gamma r) = -\frac{\alpha}{4\pi} \frac{e^{-\gamma r}}{\gamma r}, \quad (15b)$$

where α is defined by Eq. (6). Then, regardless of dimensionality, the effective potential in (11) reduces to the one-dimensional integral

$$\Delta\phi_{\text{eff}}(x) = -\frac{\alpha}{2} \int_0^\infty dx' e^{-1x-x'} \rho_L(x'), \quad (16)$$

where $x \equiv \gamma z$.

The convenience of this choice of the potentials becomes evident on applying d^2/dx^2 to Eq. (12).⁶ It is found that

$$\frac{d^2}{dx^2} (\mu_h^* - \mu) = \mu_h^* - \mu - \alpha \rho_L(x), \quad (17)$$

where μ_h^* denotes the local hard-sphere chemical potential $\mu_h\{\rho_L(x)\}$. Integrating the last equation with respect to the variable μ_h^* , on noting the thermodynamic relation

$$\rho_L(x) = \frac{\partial p_h^*}{\partial \mu_h^*}, \quad (18)$$

where $p_h^* \equiv p_h\{\rho_L(x)\}$ is the local hard-sphere pressure, and using Eqs. (5) and (7) for the asymptotic ($x \rightarrow \infty$) uniform fluid, we obtain

$$\left(\frac{d}{dx} \mu_h^*\right)^2 = \psi(x), \quad (19)$$

where

$$\psi(x) = (\mu_h^* - \mu)^2 - 2\alpha(p_h^* - p). \quad (20a)$$

Applying also the "local" versions of (5) and (7), $\psi(x)$ can be expressed in the alternative form

$$\psi(x) = (\mu^* - \mu)^2 + 2\alpha\rho_L(x)(\mu^* - \mu) - 2\alpha(p^* - p), \quad (20b)$$

with μ^* and p^* denoting respectively the local values of the total chemical potential and pressure. Finally, by regarding $\rho_L(x)$ and the local pressure, and therefore $\psi(x)$, as functions of the local chemical potential μ_h^* , Eq. (19) yields an implicit solution for the density profile

$$x = \int_{\mu_h^*(0)}^{\mu_h^*(x)} \frac{d\mu_h^*}{\pm [\psi(\mu_h^*)]^{1/2}}. \quad (21)$$

The choice of sign in the integrand depends on whether μ_h^* or (since the hard-sphere chemical potential is a monotonically increasing function of density) $\rho_L(x)$ is an increasing or decreasing function of x . This in turn depends on the boundary conditions determining the value $\mu_h^*(0) \equiv \mu_h\{\rho_L(0)\}$, which we shall examine shortly.

The behavior of the function $\psi(\mu_h^*)$ has been discussed previously^{5,6} in the context of the interfacial density profile between coexisting gas and liquid phases, where no constraining wall is present. In that situation, one desires a solution for $\mu_h^*(x) \equiv \mu_h\{\rho_L(x)\}$ which tends to the finite value $\mu_{h,g} \equiv \mu_h(\rho_g)$ as $x \rightarrow +\infty$ (or $x \rightarrow -\infty$), and to the finite value $\mu_{h,l} \equiv \mu_h(\rho_l)$ as $x \rightarrow -\infty$ (or $x \rightarrow +\infty$), where ρ_g and ρ_l are respectively the densities of the coexist-

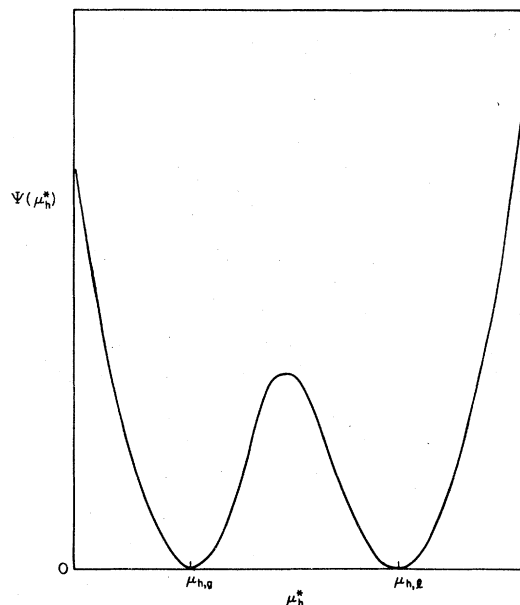


FIG. 1. Behavior of the function $\psi(\mu_h^*)$ in the presence of coexisting gas and liquid phases.

ing gas and liquid phases. In view of (21), this requires that $\psi(\mu_h^*)$ have the form shown in Fig. 1, with equal minima $\psi = 0$ at $\mu_{h,g}$ and $\mu_{h,l}$. It is readily seen from (20a) or (20b) that the vanishing of $\psi(\mu_h^*)$ and its slope at $\mu_{h,g}$ and $\mu_{h,l}$ corresponds to the equality of the total chemical potentials and pressures of the coexisting phases, i.e.,

$$\begin{aligned} \mu(\rho_g) &= \mu(\rho_l) = \mu, \\ p(\rho_g) &= p(\rho_l) = p. \end{aligned} \quad (22)$$

With a wall present at $x = 0$ to induce nonuniformity, it is no longer necessary that the asymptotic bulk density ρ at $x \rightarrow \infty$ be taken equal to one of the coexisting values ρ_g or ρ_l . Let us consider in particular the behavior of $\psi(\mu_h^*)$ when ρ is slightly less than ρ_g for the temperature in question, corresponding to adsorption from a subcritical vapor. Typically in this case, $\psi(\mu_h^*)$ has the form shown in Fig. 2, constructed using the hard-sphere functions μ_h^* and p_h^* discussed in the following section. There is of course still a minimum $\psi = 0$ at $\mu_h \equiv \mu_h\{\rho\}$, giving in (21) the required asymptotic solution $\rho_L(x) \rightarrow \rho$ as $x \rightarrow \infty$. A second minimum $\psi^* > 0$ is also present at $\mu_h^* \equiv \mu_h\{\rho^*\}$. As the bulk density ρ is decreased away from ρ_g , one finds that this second minimum gradually disappears, while as ρ is increased toward ρ_g , $\psi(\mu_h^*)$ must approach the form shown in Fig. 1. Hence, in the limit as $\rho \rightarrow \rho_g$, we have $\psi^* \rightarrow 0$ and $\mu_h^* \rightarrow \mu_{h,l}$.

It is now apparent that three different types of behavior can be obtained in the limit $\rho \rightarrow \rho_g$, depending on whether in this limit $\mu_h^*(0) < \mu_{h,g}$, $\mu_{h,g}$

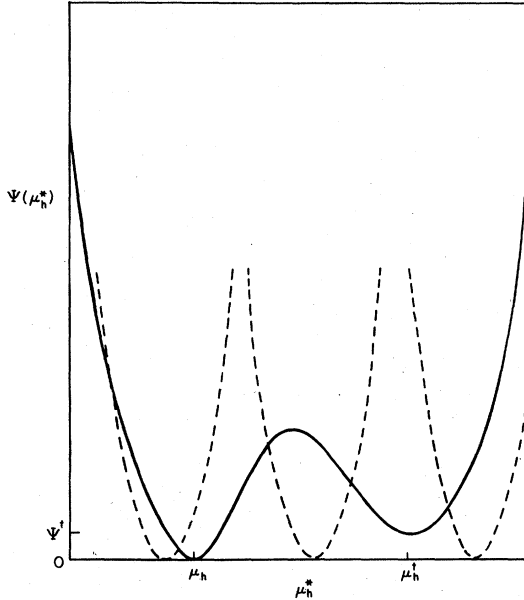


FIG. 2. Behavior of $\psi(\mu_h^*)$ (solid line) when the asymptotic density ρ is slightly less than the value ρ_g for a saturated vapor. Dashed curves show the function $I(\mu_h^*)$, Eq. (26), for three values of ϵ_w , increasing from left to right, corresponding to incipient formation of class-III, -II, and -I films.

$\mu_h^*(0) < \mu_h^\dagger$, or $\mu_h^\dagger < \mu_h^*(0)$. In the first case, the density profile determined by (21) must increase monotonically (+ sign in integrand) from $\rho_L(0)$ at the origin to the bulk value ρ as $x \rightarrow \infty$. Since $\rho_L(x) < \rho$ for all x , the contribution of $\rho_L(x)$ to the coverage

$$\theta_L \equiv \int_0^\infty dx [\rho_L(x) - \rho] \quad (23)$$

is in this case a negative quantity and remains finite in the limit $\rho \rightarrow \rho_g$.²¹ The resulting adsorption isotherms conform to class-III behavior.¹⁻³ In practice, negative coverage cannot be measured by conventional techniques,²² so only the absence of positively adsorbed amounts is observed. In principle the coverage also has a contribution from the short-range part of the density profile, cf. (10) and (13), which for hard-sphere models is intrinsically positive.^{20,23} In the strict $\gamma \rightarrow 0$ limit, however, the short-range contribution to the coverage is negligible compared with θ_L .

When $\mu_h^*(0)$ is fixed by the boundary conditions so that $\mu_h < \mu_h^*(0) < \mu_h^\dagger$, the density profile obtained from (21) decreases monotonically for all x . As in the class-III case discussed above, the integrand of (21) becomes singular only as $\mu_h^* \rightarrow \mu_h$. In other words, $x \rightarrow \infty$ only as the upper limit of integration in (21), $\mu_h^*(x)$, approaches the bulk value μ_h . In this case, the coverage θ_L is positive and remains

finite as $\rho \rightarrow \rho_g$, implying class-II behavior. In contrast, when $\mu_h^\dagger < \mu_h^*(0)$, the path of integration in (21) passes through the minimum ψ^\dagger . If this condition persists in the limit $\rho \rightarrow \rho_g$, where $\mu_h^\dagger \rightarrow \mu_{h,i}$ and $\psi^\dagger \rightarrow 0$, the singularity at μ_h^\dagger is encountered before that at μ_h . Therefore $x \rightarrow \infty$ as $\rho_L(x) \rightarrow \rho$, corresponding to condensation of an infinitely thick film of liquid density on the wall. This leads to infinite coverage θ_L in the limit $\rho \rightarrow \rho_g$, the signature of class-I behavior.

The boundary conditions fixing the value of $\mu_h^*(0)$ are easily obtained. By differentiating once with respect to x at $x=0$, we find from (14) and (16)

$$\begin{aligned} \phi_L'(0) &= -\phi_L(0), \\ \Delta\phi_{\text{eff}}'(0) &= \Delta\phi_{\text{eff}}(0). \end{aligned} \quad (24)$$

Hence, taking the derivative of Eq. (12) at $x=0$ yields

$$\left(\frac{d\mu_h^*}{dx}\right)_{x=0} = \mu_h^*(0) - \mu - 2\epsilon_w, \quad (25)$$

where $\phi_L(0) = -\epsilon_w$ follows from (14). This relation, together with (19) at $x=0$, provides simultaneous equations for determining $\mu_h^*(0)$. Equivalently, $\mu_h^*(0)$ is given by the intersection of the graph of $\psi(\mu_h^*)$ with that of the function

$$I(\mu_h^*) \equiv (\mu_h^* - \mu - 2\epsilon_w)^2, \quad (26)$$

as illustrated in Fig. 2 for three different values of ϵ_w . It is clear from the last equation that the solution for $\mu_h^*(0)$ so obtained increases as ϵ_w increases, as one expects intuitively, so that the behavior of the solution passes in order through classes III, II, and I with increasing ϵ_w . Note that, as seen in Fig. 2, there can be two intersections of $I(\mu_h^*)$ with $\psi(\mu_h^*)$. However, $(d\mu_h^*/dx)_{x=0}$ is required to be positive when $\mu_h^*(0) < \mu_h$, and negative when $\mu_h^*(0) > \mu_h$. Thus, in view of (25), only the larger solution for $\mu_h^*(0)$ is allowed when the intersections occur at values smaller than μ_h , while the smaller solution must be taken when the intersections occur at values greater than μ_h .

The particular class in which a given substrate-fluid system falls is thus determined by the value of $\mu_h^*(0)$ relative to the values μ_h and μ_h^\dagger at the minima of ψ , in the limit $\rho \rightarrow \rho_g$. In this limit, where $\mu_h^\dagger \rightarrow \mu_{h,i}$ and $\mu_h \rightarrow \mu_{h,g}$, class-I films are obtained if $\mu_h^*(0) > \mu_{h,i}$, class-II films if $\mu_{h,g} < \mu_h^*(0) < \mu_{h,i}$, and class-III films if $\mu_h^*(0) < \mu_{h,g}$. If, for a given system, the value $\mu_h^*(0)$ corresponds exactly to one of the minima $\mu_{h,g}$ or $\mu_{h,i}$ in the limit $\rho \rightarrow \rho_g$, then there will be incipient crossover between two different classes. But in these circumstances, $\psi(\mu_h^*(0)) = 0$, and therefore from (25)

$$\mu_h^*(0) - \mu - 2\epsilon_w = 0, \quad (27)$$

from which the conditions for crossover are easily found. Let us rewrite this equation, using (5), as

$$\mu^*(0) - \mu + [\alpha\rho_L(0) - 2\epsilon_w] = 0 \quad (28)$$

where $\mu^*(0) \equiv \mu\{\rho_L(0)\}$. Both at the crossover between classes III and II and, in view of the equality of chemical potentials in (22), at the crossover between classes II and I, $\mu^*(0) = \mu$, so that the last equation gives

$$\frac{2\epsilon_w}{\alpha} = \begin{cases} \rho_L(0) \\ \rho_g \text{ (class III-class II)} \\ \rho_l \text{ (class II-class I)}. \end{cases} \quad (29)$$

From this result, the temperature at which a given system changes classes can be obtained. From Eq. (6), the parameter α is equal to the integrated strength of intermolecular attractions and is thus proportional to the familiar Van der Waals a parameter. Alternatively, as shown in the following section, α can be taken proportional to the well depth ϵ in a *realistic* model (e.g., Lennard-Jones) for pair interactions between the molecules. The variation of ρ_g and ρ_l with temperature is of course the coexistence curve: This will be roughly of universal character if plotted in terms of the reduced temperature $T^* \equiv kT/\epsilon$, where k is Boltzmann's constant. Thus we have derived a crossover curve, having the same shape as the coexistence curve and of approximately universal nature, for the crossover temperature as a function of the ratio ϵ_w/ϵ . This is shown schematically in Fig. 3 and justifies our statement at the beginning that a given system, characterized by ϵ_w/ϵ , will at some point change from class II to either class I or class III with increase in temperature.

We remark in passing that analogous results are found in the case of adsorption from a *dense* fluid, that is, where the asymptotic density ρ is greater than ρ_l . For values of ρ close to ρ_l , the behavior of $\psi(\mu_h^*)$ is similar to that shown earlier in Fig. 2, having two minima $\psi = 0$ at μ_h and $\psi^\dagger > 0$ at μ_h^\dagger , where now $\mu_h^\dagger < \mu_h$. In the limit $\rho \rightarrow \rho_l$, the minimum ψ^\dagger approaches zero and μ_h^\dagger approaches the value $\mu_{h,g}$, so that we can again speak of three classes of behavior. There are, however, some major differences from the case of adsorption from a vapor, if we retain our earlier classification, namely class I if $\mu_h^*(0) > \mu_{h,l}$, class II if $\mu_{h,g} < \mu_h^*(0) < \mu_{h,l}$, and class III if $\mu_h^*(0) < \mu_{h,g}$. Now both classes III and II give negative coverage in the limit $\rho \rightarrow \rho_l$, with θ_L for class III becoming infinitely negative in this limit, while θ_L for class I is positive and remains finite in the limit. We are not aware of any experimental studies with which to check this picture.

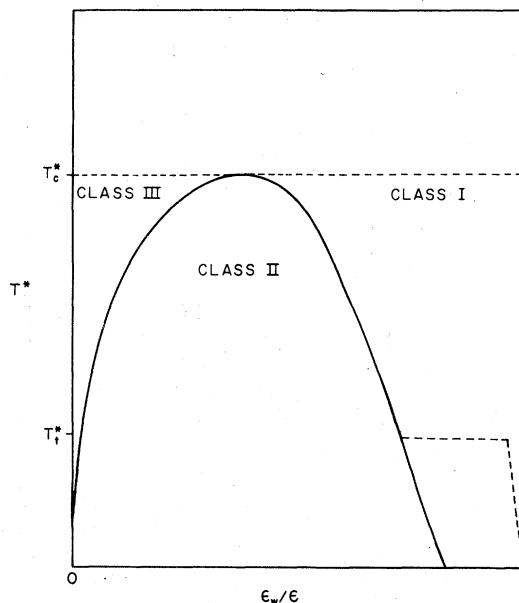


FIG. 3. Schematic "crossover curve" given by the present model (solid line). Dashed line shows conjectured modification, Eq. (35), of the boundary between classes II and I below the reduced triple-point temperature $T_t^* \equiv kT_t/\epsilon$.

IV. EXAMPLES

In this section we use Eq. (29) to estimate crossover temperatures for rare gases adsorbed on a number of substrates. To do so requires evaluation of α as well as knowledge of the coexistence curve. Both are achieved here by adopting the accurate Carnahan-Starling²⁴ expression for the hard-sphere pressure,

$$p_h(\rho) = \rho kT(1 + \eta + \eta^2 - \eta^3)/(1 - \eta)^3, \quad (30)$$

where $\eta \equiv \pi\rho\sigma^3/6$ with σ the hard-sphere diameter. Using the relation $\partial p_h/\partial\rho = \rho\partial\mu_h/\partial\rho$, the configurational part of the chemical potential is found to be

$$\mu_h(\rho) = kT[\ln(\eta) + \eta(8 - 9\eta + 3\eta^2)/(1 - \eta)^3]. \quad (31)$$

For specified α , use of these relations in the generalized⁴ Van der Waals expressions (5) and (7) enables us, on applying the equality of pressures and chemical potentials Eq. (22), to numerically determine the coexistence curve for the model fluid.

The critical density ρ_c and temperature T_c can also be obtained by solving

$$\frac{\partial p}{\partial\rho} = \frac{\partial^2 p}{\partial\rho^2} = 0 \text{ at } \rho_c \text{ and } T_c,$$

which results in the values

$$\begin{aligned} \rho_c\sigma^3 &= 0.249, \\ \alpha/kT_c\sigma^3 &= 11.102. \end{aligned} \quad (32)$$

To fit the model coexistence curve to experiment, we proceed here, arbitrarily but simply, by using the second relation in (32) to determine values for α/σ^3 from given values for the critical temperature. Also, substituting for α from (32) into (29) and dividing through by ϵ , the latter equation can be written

$$\epsilon_w/\epsilon = 5.551 T_c^* \rho_x \sigma^3, \quad (33)$$

where $T_c^* = kT_c/\epsilon$, and $\rho_x = \rho_l$ or ρ_g for crossover between classes I and II or between classes II and III, respectively. Note that if the coexistence curve were indeed universal, T_c^* would be the same for all adsorbates. Thus variation in T_c^* indicates the degree of nonuniversality.

The procedure now is to use (33) to estimate $\rho_x \sigma^3$ from knowledge of ϵ_w , ϵ , and T_c for a given fluid/substrate pair. From the coexistence curve for the fluid constructed as described above, the corresponding crossover temperature can be read off. Clearly, if the predicted value of $\rho_x \sigma^3$ is greater than $\rho_c \sigma^3$, the transition will be between classes II and I; otherwise, it will be between classes II and III.

This method will be applied to the gases argon, krypton, and xenon adsorbed on graphite. The parameter ϵ_w is taken equal to the minimum in the gas-graphite potential, for which reliable estimates are available,^{22,25} while ϵ is identified with the minimum in the standard Lennard-Jones (6-12) model for the pair potential of the gas. Adsorption isotherms of Ar on graphite which has been coated with several layers of Xe have also been reported,¹¹ showing a class-II-class-I transition. We approximate this system by the adsorption of Ar on pure solid Xe. Again, the relevant gas-substrate potential parameters are available.²⁵ Finally, we consider a model for Ar adsorbed on solid carbon dioxide, which has recently been studied by Monte Carlo methods.¹² We make use of the same potential parameters ϵ , ϵ_w as this study and

note that the appropriate critical temperature should not be taken as the experimental value for Ar but rather the value for a model Lennard-Jones fluid, $T_c^* = 1.32$.^{26,27}

The parameters used and the resulting estimates for the crossover temperatures T_x are given in Table I.^{28,29} Immediately it is noted that the predicted T_x for all but the last adsorbate are below the corresponding triple-point temperatures T_t and that the crossover densities $\rho_x \sigma^3$ [equal to the density in contact with the surface, cf. (29)] for the first three adsorbates are well into the normal solid regime. The existence of solid phases exhibiting a triple point is of course not included in our model. To encompass such features requires an adequate theory of crystallization, at present unavailable. Thus the interpretation of these results is somewhat uncertain. Nonetheless, the predicted crossover temperatures for rare gases on graphite are consistent with the fact that these systems exhibit class-I behavior at the temperatures used in existing measurements; $T = 77^\circ$ for Ar (Ref. 30) and Kr (Ref. 31), $T = 109^\circ$ for Xe (Ref. 31), all of which are still below the corresponding triple points. The predicted crossover temperature for Ar on Xe, $T_x = 75^\circ$, agrees closely with the experimental results,¹¹ which indicate a transition between 79° and 81° . For the latter system, some adsorption isotherms which span the theoretical crossover region are shown in Fig. 4. These have been calculated using (19) and (23), from which θ_L can be expressed as

$$\theta_L = \int_{\mu_h^*(0)}^{\mu_h} \frac{\rho_L(\mu_h^*) - \rho}{\pm [\psi(\mu_h^*)]^{1/2}} d\mu_h^*, \quad (34)$$

requiring a single numerical quadrature. The resulting isotherms in Fig. 4 exhibit qualitatively the same form as found experimentally.¹¹

The ambiguity due to exclusion of solid phases from the present model does not apply to the final

TABLE I. Predicted crossover temperatures T_x for rare gases on several substrates.

	ϵ/k (°K)	ϵ_w/k (°K)	T_c (°K)	T_c^*	T_t (°K)	ϵ_w/ϵ	$\rho_x \sigma^3$	T_x (°K)
Xe-graphite	221 ^a	1919 ^b	290 ^c	1.31	161 ^e	8.68	1.19	58
Kr-graphite	171	1460	209	1.22	116	8.54	1.26	32
Ar-graphite	120	1107	151	1.26	84	9.23	1.32	18
Ar-graphite	120	730 ^c	151	1.26	84	6.08	0.87	75
Ar-CO ₂	120	334 ^d	158 ^f	1.32 ^f		2.78	0.38	153

^aReference 29.

^bReference 22, p. 174.

^cReference 25, p. 45.

^dReference 13.

^eReference 28.

^fReference 26.

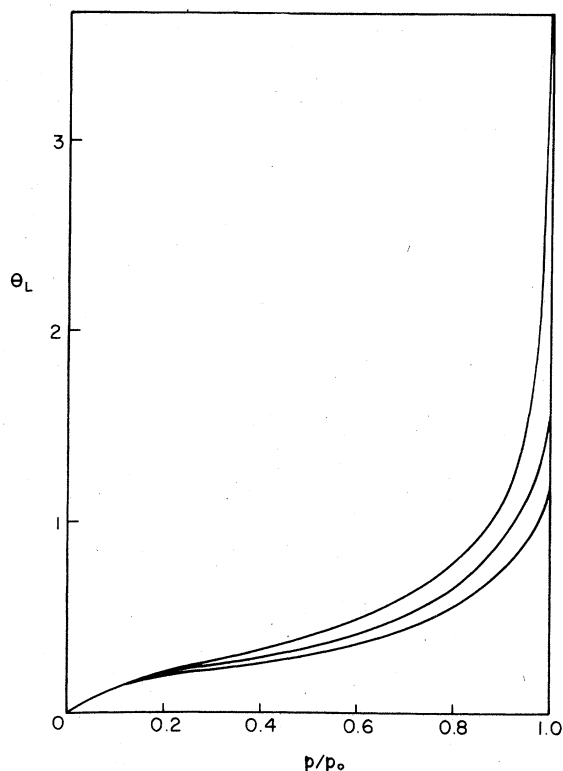


FIG. 4. Calculated adsorption isotherms using the Ar-Xe parameters of Table I. From top to bottom, $T^* = 0.65$ (class I), 0.60, and 0.57. The axis is labeled by the ratio of the pressure to the saturated vapor pressure ρ_0 for each temperature.

system in Table I. Indeed, due to the weak surface-molecule attractions in this case, manifest in the relatively small value of ϵ_w/ϵ , the predicted class-II-class-I transition does not occur until the temperature is very close to the critical point. This is consistent with the results of Monte Carlo simulations of this system,¹² which show no evidence of unlimited film growth at reduced temperatures $T^* = 0.9$ and $T^* = 1.1$, implying the formation of class-II films at these temperatures.

V. DISCUSSION

In this paper we have developed a model for non-uniform fluids in the presence of solid substrates, based on Van der Waals's original concept of dividing the interaction potential between a pair of molecules into a short-range repulsive part and a long-range attractive part. Here this concept was generalized to treat the interaction between the fluid molecules and the substrate. The Van der Waals model predicts clearly the existence of three classes of film-growth behavior, with a crossover curve between different classes that is simply related to the phase coexistence curve.

The examples discussed in the last section are certainly in accord with this description, although the picture is clouded by the model's inability to account for solid-fluid transitions. We can speculate, nonetheless, on the possible modifications of the crossover equation (29) when such transitions are included. Below the triple point, the only stable bulk phases are gas and solid, so we might expect that the condition for crossover between classes II and I in (29) should be replaced by

$$\frac{2\epsilon_w}{\alpha} = \begin{cases} \rho_l, & T_x > T_t \\ \rho_s, & T_x < T_t, \end{cases} \quad (35)$$

where T_t is the triple-point temperature and ρ_s is the density of solid in equilibrium with vapor at temperature T_x . This would then lead to the modification of the crossover curve shown by the dashed line in Fig. 3. In particular, there would be a range of values ϵ_w/ϵ over which the crossover temperature remains constant at the value T_t , which could explain why a number of substances^{9,10} appear to change classes at precisely this temperature. For the present, however, this remains a conjecture.

Besides its present limitation to describing disordered fluid phases, the model is strictly applicable only in the unrealistic limit that the attractive forces are infinitely slowly varying. However, the results may be expected to have at least the same qualitative validity as Van der Waals's equation of state for bulk fluids. In addition, there are available⁴ several methods for systematically extending the model to higher order in the inverse range parameter γ . Probably the most significant feature that will emerge in such an extension is the coupling of the short-range and long-range parts of the density profile: As noted at the end of Sec. II, in the present model the long-range part is independent of short-range correlations. We anticipate that this coupling will be necessary to account for such effects as phase transitions in the monolayer regime.³² We defer this extension to later work.

An alternative to formal γ -expansion techniques for improving on the basic Van der Waals model would make use of integral-equation methods similar to those we have discussed elsewhere.⁷ These methods are analogous to theories (e.g., Percus-Yevick, hypernetted chain) which have been successful in describing the bulk structure of liquids. An often held tenet when this approach is applied to bulk liquids, in seeking successively better approximations for the microscopic structure, is that the rapidly varying repulsive forces dominate

the structure. In view of our remarks at the end of Sec. II, this is no longer generally true when applied to the description of surface structure.²⁷ The profound effect of attractive forces was reflected in our earlier work⁷ by the large disparity between the results of different integral-equation approximations, none of which, it was noted, agree with the local thermodynamic relation (12) in the $\gamma \rightarrow 0$ limit. However, it is possible to incorporate local thermodynamics in the integral-equation approach, and hence recover Van der Waals's model in the $\gamma \rightarrow 0$ limit, by use of an "effective density" technique.³³ Here the full density profile is determined by an equation similar to (12), but where the local hard-sphere chemical potential is evaluated at a local effective density which is some weighted average of $\rho(z)$ including the effects of short-range correlations. The details of this approach will be published later.

Finally, we comment on the "density-functional" theory of Ebner and Saam.^{13,14} It was pointed out in Ref. 12 that Monte Carlo simulations of the Ar-CO₂ system at reduced temperatures $T^* = 0.9$ and 1.1 show no evidence of unlimited film growth (i.e., class-I behavior), contradicting the density-functional theory, which predicts such growth. Now the latter theory, as well as several others proposed recently,^{15,16} attempt in various ways to incorporate local thermodynamics. It is instructive to consider the $\gamma \rightarrow 0$ limit of these theories, where it is found that the long-range density profile is determined by

$$\mu - \phi_L(x) = \mu\{\rho_L(x)\}, \quad x > 0, \quad (36)$$

using the notation of this paper. Comparing this equation with (13), one sees that (36) results essentially on making a local approximation to the effective potential $\Delta\phi_{\text{eff}}(x)$. In applying (36), one faces the problem of evaluating the total chemical potential $\mu\{\rho_L(x)\}$ at local densities $\rho_L(x)$ which may occur in the bulk two-phase regions. (Still greater difficulties are encountered in the com-

plete versions of these theories, which require evaluating bulk pair correlation functions at local densities which may lie in unphysical regions of the corresponding bulk phase diagram.) If isotherms of $\mu\{\rho_L(x)\}$ are given by the usual Maxwell construction, i.e., with a horizontal line in the two-phase region, then the implications of (36) are clear: The density profile $\rho_L(x)$ undergoes a jump discontinuity from ρ_l to ρ_g at the position x^\dagger satisfying

$$\mu - \phi_L(x^\dagger) = \mu(\rho_g), \quad (37)$$

where $\mu(\rho_g) = \mu(\rho_l)$ is the common chemical potential of coexisting gas and liquid phases. As the density of the asymptotic uniform vapor approaches ρ_g , so that $\mu \rightarrow \mu(\rho_g)$, the position x^\dagger must approach infinity, signifying unlimited growth of a liquid film on the surface. This process occurs for any long-range attractive potential $\phi_L(x)$, no matter how weak, with the consequence that (36) *always* predicts class-I film formation. While higher-order terms in the density-functional theories will serve to smooth out the discontinuity in the density profile at x^\dagger , they will not mitigate the basic fault of these theories, namely that the effects of attractive pair interactions are included from the outset in local thermodynamic functions such as $\mu\{\rho_L(x)\}$. In short, these theories do not follow Van der Waals' in clearly distinguishing the roles of short-range repulsive potentials and long-range attractive interactions.

ACKNOWLEDGMENTS

The financial support of the Research Advisory Board of the University of Guelph, and of the Natural Sciences and Engineering Research Council, is gratefully acknowledged. The author is indebted to Professor G. Stell for his continued encouragement, interest, and suggestions for this work, and to Professor N. G. Van Kampen for several valuable discussions during his timely visit to Guelph.

¹J. G. Dash, Phys. Rev. B **15**, 3136 (1977).

²J. G. Dash, J. Phys. (Paris) **38**, C4, 201 (1977).

³R. Peierls, Phys. Rev. B **18**, 2013 (1978).

⁴P. C. Hemmer and J. L. Lebowitz, in *Phase Transitions and Critical Phenomena*, edited by C. Domb and M. S. Green (Academic, New York, 1976), Vol. VB.

⁵N. G. Van Kampen, Phys. Rev. **135**, A362 (1964).

⁶J. K. Percus, Trans. N. Y. Acad. Sci. **26**, 1062 (1964); Lecture Notes on Nonuniform Fluids [Enseignement de 3ème Cycle de Physique en Suisse Romande, Lausanne, 1975 (unpublished)].

⁷(a) D. E. Sullivan and G. Stell, J. Chem. Phys. **69**, 5450 (1978); (b) *ibid.*, Appendix. In this reference, $\phi_{\text{eff}}(\vec{r})$

is the same as the present function $\phi_{\text{eff}}(\vec{r}) + \alpha\rho$.

⁸M. J. de Oliveira and R. B. Griffiths, Surf. Sci. **71**, 687 (1978).

⁹J. W. White, R. K. Thomas, T. Trewern, I. Marlow, and G. Bomchil, Surf. Sci. **76**, 13 (1978).

¹⁰J. Menaucourt, A. Thomy, and X. Duval, J. Phys. (Paris) **38**, C4, 195 (1977).

¹¹C. F. Prenzlow and G. D. Halsey, Jr., J. Phys. Chem. **61**, 1158 (1957).

¹²J. E. Lane, T. H. Spurling, B. C. Freasier, J. W. Perram, and E. R. Smith (unpublished).

¹³C. Ebner and W. F. Saam, Phys. Rev. Lett. **38**, 1486 (1977).

- ¹⁴W. F. Saam and C. Ebner, *Phys. Rev. A* **17**, 1768 (1978).
- ¹⁵Y. Singh and F. F. Abraham, *J. Chem. Phys.* **67**, 537 (1977); **67**, 5960 (1977).
- ¹⁶V. Bongiorno and H. T. Davis, *Phys. Rev. A* **12**, 2213 (1975).
- ¹⁷J. L. Lebowitz and J. K. Percus, *J. Math. Phys.* **4**, 116 (1963).
- ¹⁸C. S. Simmons and C. Garrod, *J. Math. Phys.* **14**, 1075 (1973).
- ¹⁹D. Henderson, F. F. Abraham, and J. A. Barker, *Mol. Phys.* **31**, 1291 (1976).
- ²⁰E. Waisman, D. Henderson, and J. L. Lebowitz, *Mol. Phys.* **32**, 1373 (1976).
- ²¹Strictly, negative coverage θ_L need only be obtained in the limit $\rho \rightarrow \rho_g$ to signify class-III behavior. For smaller values of ρ , the present model may give positive (but very small) values for θ_L , the resulting adsorption isotherms showing a maximum. In the limit $\epsilon_w \rightarrow 0$, however, the boundary conditions discussed here give $p_h\{\rho_L(0)\} = p$ (see also Ref. 7b), which can be shown to imply $\rho_L(0) < \rho$ for any ρ .
- ²²R. A. Pierotti and H. E. Thomas, in *Surface and Colloid Science*, edited by E. Matijevic (Wiley, New York, 1971), Vol. IV.
- ²³D. Henderson, *J. Chem. Phys.* **68**, 780 (1978).
- ²⁴N. F. Carnahan and K. E. Starling, *Phys. Rev. A* **1**, 1672 (1970).
- ²⁵W. A. Steele, *The Interaction of Gases with Solid Surfaces* (Pergamon, New York, 1974).
- ²⁶J. A. Barker and D. Henderson, *Rev. Mod. Phys.* **48**, 587 (1976).
- ²⁷Since long-range attractive pair forces have a major influence on surface structure, the results of computer simulations of surfaces must be interpreted carefully. Specifically, the Lennard-Jones pair potential in a computer simulation is always truncated at a finite distance. The results for the surface structure will then generally differ from those expected using an untruncated potential [J. J. Weis, D. E. Sullivan (unpublished)]. In view of this, the effective critical temperature for the simulation results of Ref. 12 should be somewhat less than the value corresponding to a full Lennard-Jones potential.
- ²⁸A. Thomy and X. Duval, *J. Chim. Phys. Phys. Chim. Biol.* **67**, 1101 (1970).
- ²⁹J. O. Hirschfelder, C. F. Curtiss, and R. B. Bird, *Molecular Theory of Gases and Liquids* (Wiley, New York, 1954).
- ³⁰J. H. Singleton and G. D. Halsey, Jr., *J. Phys. Chem.* **58**, 1011 (1954).
- ³¹A. Thomy and X. Duval, *J. Chim. Phys. Phys. Chim. Biol.* **67**, 286 (1970).
- ³²E. R. Smith and J. W. Perram, *J. Stat. Phys.* **17**, 47 (1977).
- ³³J. L. Lebowitz and E. Praestgaard, *J. Chem. Phys.* **40**, 2951 (1964).